Supernova Neutrino Spectrum with Matter and Spin Flavor Precession Effects

A. Ahriche & J. Mimouni

Physics department, Mentouri University, Route de Ain El-Bey,
Constantine 25000, Algeria.

 $E-mail: amin_ahriche@hotmail.com, jamalm@wissal.dz$

November 19, 2018

Abstract

We consider Majorana neutrino conversions inside supernovae by taking into account both flavor mixing and the neutrino magnetic moment. We study the adiabaticity of various possible transitions between the neutrino states for both normal and inverted hierarchy within the various solar neutrino problem solutions. From the final mass spectrum within diffrent scenarios, we infer the consequences of the various conversion effects on the neutronization peak, the nature of final spectra, and the possible Earth matter effect on the final fluxes. This enable us to check the sensibility of the SN neutrino flux on magnetic moment interaction, and narrow down possible scenarios which depend on: the mass spectrum normal or inverted, the solution of the solar neutrino problem; and the value of μB .

1 Introduction

The neutrino signal detected on the Earth from the SN1987A explosion [1] has opened up new ways to probe the neutrino properties. Initially only constraints on the static properties of neutrino during its interstellar journey (namely from vacuum oscillations) could be acquired. Now with the entry into service of the large neutrino underground detectors like Superkamiokande (SK) [2] and the Sudbury Neutrino Observatory (SNO) [3], modification of the flavor content of the neutrinos emerging from the SN itself could be contemplated. This is helped greatly by the new quantitative progress achieved in the past few years in our knowledge of the mass squared differences and mixing parameters from the atmospheric neutrino oscillations (SK and MACRO [4] in particular), and the solar neutrino oscillations [5].

Various works have appeared studying the consequences of both the matter resonance effect (the so called MSW effect) [6], and the spin flavor precession (the RSFP effect) [7], especially with the present data on the neutrino magnetic moment [8], due to the very large magnetic field in the pre-supernova interior [9]. These studies have been mostly confined to the case of two active neutrinos. The case of sterile neutrinos is no more rigorously pursued in the light of the strong constraints on their existence

from the atmospheric neutrinos experiments. They used to be invoked in neutrino conversion, in particular for their potential role in enabling r-process nucleosynthesis [10].

We wish in this paper to consider the general case of three active neutrinos on the neutrino SN spectrum, namely the ones associated with the three known leptonic flavors, in the context of both the MSW effect and the RSFP effect. We have followed the seminal work of Dighe and Smirnov [11] as far as their general line of attack on the question, but generalizing it to take into account both of the above mentioned effects at the same time. Considering the various schemes of neutrino mass and mixing allowed by the data, we systematize the discussion of the various spectrum distortion effects, and thus check the discriminating power of such studies and how they could help resolve the ambiguities associated with it, notably:

- the solar neutrino solution (which one to choose?)¹.
- the type of hierarchy for the neutrino masses (normal or inverted).
- the value of μB_{\perp} where μ is the neutrino magnetic moment, and B_{\perp} the SN transverse magnetic field.

It follows from the existing solar and atmospheric neutrino data that neutrino mass-squared differences satisfy the hierarchy $\Delta m_{21}^2 \ll \Delta m_{32}^2$, which permits us to order the three mass-squared according to the two following cases: (i) normal (or direct) hierarchy, where $m_1^2 \leq m_2^2 \ll m_3^2$, and thus Δm_{32}^2 will be positive (See Fig.1-a). (ii) the inverted mass hierarchy, where $m_3^2 \ll m_1^2 \leq m_2^2$ and thus Δm_{32}^2 will be negative (See Fig.1-b). We will assume that Δm_{21}^2 is relevant for the solar neutrinos oscillations, while Δm_{32}^2 is relevant for the oscillations of the atmospheric neutrinos.

The effects of the neutrino conversions can be observed through, (i) the disappearance (partial or complete) of the neutronization peak; (ii) the interchange of original spectra and the appearance of a hard ν_e spectrum; (iii) the modification of the $\bar{\nu}_e$ spectrum; (iv) the Earth matter effect, which is studied taking into account neutrino mass and mixing in [11]. Note that for significantly cosmological mass-squared differences ($\Delta m^2 = 1 \sim 100 \text{ eV}^2$), the spin-flavor precession and resonant spin-flavor conversions may affect the supernova shock reheating and r-process nucleosynthesis [9].

Although the ambiguities on the neutrino spectrum could not be solved, a systematic study of their effects in the general three-generation case pave the way for further constraining the various scenarios as new limits are obtained from the detectors on the Earth.

This paper is organized as follows: we first obtain the original neutrino fluxes emerging from the SN core; we then study neutrino conversion outside the core for both normal and inverted mass hierarchy, and finally determinate the final neutrino fluxes which reach the Earth detectors. The various neutrino conversion effects are then classified according to the different parameters relevant for the Solar neutrino solutions and the magnitude of the magnetic interaction term μB_{\perp} .

¹The recent results from the KamLAND experiment [12] indicate that the LOW scenario is most probably ruled out, which leaves the LMA as the most favored one.

Fig 1: Neutrino mass pattern: a) represents the case within normal mass hierarchy; and b) represents the case within inverted mass hierarchy.

2 The Original Spectrum

When the inner iron core of a massive star going through a type *II* supernova explosion becomes unable to support the electron degeneracy pressure, most of the gravitational binding energy is released in the form of a violent burst of neutrinos of all species [13, 14].

These neutrinos produced both during the neutronization burst and the subsequent thermal cooling could undergo transformation of kind both inside the SN, and outside on their way to the Earth. We are however interested only in their transformation within the SN. In some scenarios these transformations could boost the energy deposition at the stalled explosion front as well as play a key role in the explosive nucleosynthesis [15]. Yet, since in our study we are using mass differences relevant to the Solar Neutrino Problem (SNP) and the Atmospheric Neutrino Problem only, these neutrinos transformations are not expected to change the dynamics of the explosion as the corresponding resonances take place outside the core.

Two effects have been widely considered: the first one is the matter effect, i.e. the interaction of ν 's with different matter constituents which are mainly electrons, protons and neutrons. The second one consists of the interaction of the neutrino's magnetic moment with the transverse magnetic field of the SN. For Dirac neutrinos, they flip into a right handed ν_R kind which is known to be sterile since undetected till now. Comparing the inferred energy output of SN1987A to the theoretical expectations, one can put strong constraints on these Dirac neutrino conversions. On the other hand, when including the most general mass terms in the simplest extension of the Weinberg-Salam model, the neutrino fields, once diagonalized, turn out to be of Majorana kind. All this concurs to make the Majorana neutrinos more palatable than the Dirac kind in the context of SN studies. We will assume in what follows that the neutrinos are Majorana particles. Now since they are their own antiparticles, only flavor conversion will be allowed.

In order to study these effects together, we should identify the profile of both the density and the SN magnetic field. We take the standard parametrization:

$$B(r) = B_{\perp o} \left(\frac{r}{r_o}\right)^{-k}; \ r \ge r_o \tag{1}$$

where $B_{\perp o}$ is the magnetic field strength at the distance $r_o=10\,\mathrm{km}$; and k=2 or 3; in our work, we will consider k=3. The value of $B_{\perp o}$ lies between² $\left(10^{12}\sim10^{15}\right)G$, where G is the strength magnetic field unit. For this density profile, the important effects occur between³ $O(1\mathrm{g\,cm^{-3}})$ and $O(10^7\,\mathrm{g\,cm^{-3}})$, i.e. this region may not be affected by the SN shock wave. We will thus take the progenitor profile for $\rho \gtrsim 1\,\mathrm{g\,cm^{-3}}$ as approximately given by [17]

$$\rho Y_e \approx \rho_o \left(\frac{r}{r_o}\right)^{-3} \tag{2}$$

where $\rho_o = 2 \times 10^{13} \,\mathrm{g\,cm^{-3}}$. Of course, the exact shape of the density profile will depend on the precise composition of the star.

The first question to answer is the flavor content of this burst when reaching the conversion regions. The key point here is that they are produced in a high density medium so that their mass eigenstates can readily be inferred.

For this matter, let us rewrite the Hamiltonian in the flavored basis $\nu^f = (\nu_e, \nu_\mu, \nu_\tau, \bar{\nu}_e, \bar{\nu}_\mu, \bar{\nu}_\tau)$ which is related to the mass eigenstates basis in vacuum $\nu^v = (\nu_1, \nu_2, \nu_3, \bar{\nu}_1, \bar{\nu}_2, \bar{\nu}_3)$ by the unitary transformation $\nu^f = U\nu^v$. We can then deduce the initial mass spectrum from the evolution of neutrinos at very high density $(\rho \gtrsim 10^8 \text{ g cm}^{-3})$.

Taking into account the neutrino effective potential coming from both the MSW effect and the RSFP effect, we can cast the Hamiltonian into the following form:

$$H = \text{Vacuum term} + \text{Matter term} + \text{Spin Precession term}$$
 (3)

where each term, after the substraction of terms proportional to the unity, is given by:

Vacuum term =
$$\frac{1}{2E} \begin{pmatrix} U & 0 \\ 0 & U \end{pmatrix} \begin{pmatrix} M^2 & 0 \\ 0 & M^2 \end{pmatrix} \begin{pmatrix} U^{\dagger} & 0 \\ 0 & U^{\dagger} \end{pmatrix}$$

Matter term = $\alpha \rho \times \text{diag} \{Y_{e}, 0, 0, 1-2Y_{e}, 1-Y_{e}, 1-Y_{e}\}$

Spin Precession term = $\begin{pmatrix} 0 & C \\ -C & 0 \end{pmatrix}$, where $C = \begin{pmatrix} 0 & \mu_{e\mu} & \mu_{e\tau} \\ -\mu_{e\mu} & 0 & \mu_{\mu\tau} \\ -\mu_{e\tau} & -\mu_{\mu\tau} & 0 \end{pmatrix} \times B_{\perp}$

(4)

with $M^2 = diag\{0, \Delta m_{21}^2, \Delta m_{31}^2\}$, $\alpha = \sqrt{2}G_F m_N$, $Y_e = \frac{n_e}{n_e + n_n}$ is the electronic fraction, the Δm^2 's are the difference between squared masses; $\mu_{e\mu}$ is the transition magnetic moment between the two flavored states ν_e and ν_μ ; and U is the mixing matrix given by [18]

$$\begin{pmatrix}
c_{12}c_{13} & s_{12}c_{13} & s_{13} \\
-s_{12}c_{23} - c_{12}s_{23}s_{13} & c_{12}c_{23} - s_{12}s_{23}s_{13} & s_{23}c_{13} \\
s_{12}s_{23} - c_{12}c_{23}s_{13} & -c_{12}s_{23} - s_{12}c_{23}s_{13} & c_{23}c_{13}
\end{pmatrix} (5)$$

²This is taken to be the transversal value of the magnetic field strength at the surface of the neutron star.

 $^{^3}$ The resonance densities are approximately given by $\sim \frac{m_N \Delta m^2 \cos 2\theta}{2\sqrt{2}G_F \, E} \frac{1}{q},$ where q is Y_e for the MSW transitions, and $1\text{-}2Y_e$ for the RSFP ones. The values of Δm^2 and θ are taken from the solar and atmospheric neutrino data. Y_e is generally set to be half, and therefore $1\text{-}2Y_e$ lies between 10^{-4} to 10^{-3} [16], then all transitions occur in a range extending from a few g.cm $^{-3}$ to 10^7 g.cm $^{-3}$.

where $s_{ij} = \sin \theta_{ij}$, $c_{ij} = \cos \theta_{ij}$ for i,j = 1,2,3 (i < j); and θ_{ij} is the vacuum mixing angle between ν_i and ν_j . The mixing matrix terms satisfy the unitarity relations: $\sum_i |U_{il}|^2 = \sum_l |U_{il}|^2 = 1$. The equality in the second term in Eq. (4), however, is only true to leading order since radiative corrections induce tiny differences between the neutral current potentials of ν_e , ν_μ and ν_τ , and in particular, results in a very small ν_μ - ν_τ potential difference $|V_\mu - V_\tau| \sim (10^{-5} \sim 10^{-4}) \times \alpha \rho$ [19].

Performing a rotation in the non-electronic subspace as $(\nu_{\mu},\nu_{\tau}) \longrightarrow (\nu_{\mu'},\nu_{\tau'})$ which diagonalizes the vacuum term and leaves the matter term invariant, while for the magnetic term, the two values $\mu_{e\mu}$ and $\mu_{e\tau}$ become nearly maximally mixed, and so whatever their values, the rotated ones will be of the same magnitude, and therefore we have $\mu_{e\mu'} \sim \mu_{e\tau'} \sim \mu$. As for the third one $\mu_{\mu\tau}$ it remains invariant. Since ν_{μ} and ν_{τ} are both produced via neutral currents only and are indistinguishable as far as their detection, we take the non-electronic original fluxes to be equivalent, so we can then write $F_{\mu}^{o} = F_{\tau}^{o} = F_{\mu'}^{o} = F_{\tau'}^{o}$.

Comparing at very high density, the values of the various Hamiltonian terms; we notice that for energies in the range of MeV, $\alpha\rho\gg\frac{\Delta m_{21}^2}{2E},\frac{\Delta m_{31}^2}{2E}$. Since we took the term μ to be between [20] $10^{-12}\mu_B$ and $10^{-10}\mu_B$, the same thing applies when we compare the matter term with the magnetic one with respect to the chosen range of $\mu B_{\perp o}$ i.e. $\alpha\rho\gg\mu B_{\perp o}$. Note that the chosen values of both μ and $B_{\perp o}$ don't affect the SNP solution. We then deduce that at the SN core, the matter term is the dominant one, and therefore the Hamiltonian is approximately diagonal

$$H \simeq \alpha \rho \times diag \{ Y_e, 0, 0, 1-2Y_e, 1-Y_e, 1-Y_e \}$$
 (6)

This means that the matter eigenstates coincide with the flavored states, and so, the neutrinos emerging from the SN core are as follow:

1- Normal Mass Hierarchy
$$\begin{array}{cccc} \widetilde{\nu}_{1}^{o} \sim \nu_{\mu'} & & \widetilde{\overline{\nu}}_{1}^{o} \sim \overline{\nu}_{e} \\ & \widetilde{\nu}_{2}^{o} \sim \nu_{\tau'} & & \widetilde{\overline{\nu}}_{2}^{o} \sim \overline{\nu}_{\mu'} \\ & & \widetilde{\nu}_{3}^{o} \sim \nu_{e} & & \widetilde{\overline{\nu}}_{3}^{o} \sim \overline{\nu}_{\tau'} \\ \\ 2\text{- Inverted Mass Hierarchy} & & \widetilde{\nu}_{1}^{o} \sim \nu_{\mu'} & & \widetilde{\overline{\nu}}_{1}^{o} \sim \overline{\nu}_{\tau'} \\ & & \widetilde{\nu}_{2}^{o} \sim \nu_{e} & & \widetilde{\overline{\nu}}_{2}^{o} \sim \overline{\nu}_{\mu'} \\ & & & \widetilde{\nu}_{3}^{o} \sim \nu_{\tau'} & & \widetilde{\overline{\nu}}_{3}^{o} \sim \overline{\nu}_{e} \end{array}$$

3 The Neutrino Flavor Dynamics

In order to find the final spectrum, we should study all possible transitions between the neutrino species. We note that these transitions occur in the *isotopically neutral region*⁴, which consists mainly of layers of 4He , ${}^{12}C$, ${}^{16}O$, ${}^{28}Si$ and ${}^{32}S$ whose nucleus have $N \simeq Z$, so that the electronic fraction Y_e will be close to half. We also consider the following parameters values which are: first, when the SNP solution is the LMA scenario, the present parameters are $\sin^2 2\theta_{\odot} = \sin^2 2\theta_{12} = 0.91$ and $\Delta m_{21}^2 = 6.9 \times 10^{-5} \,\mathrm{eV}^2$, while for the LOW scenario, we take $\sin^2 2\theta_{12} = 0.92$ and $\Delta m_{21}^2 = 1.3 \times 10^{-7} \,\mathrm{eV}^2$. Secondly, for the atmospheric data, we have $\sin^2 2\theta_{atm} = \sin^2 2\theta_{23} = 1$ and $\Delta m_{32}^2 = 2.7 \times 10^{-3} \,\mathrm{eV}^2$.

⁴The region characterized by $1-2Ye=10^{-4}\sim 10^{-3}$, is called the isotopically neutral region.

Thirdly, for the 1-3 mixing, we choose a value just below the experimental limit, which is given by CHOOZ [21], and satisfies the adiabaticity condition at the H resonance, which leads us to take $\sin^2 \theta_{13} = 10^{-3}$.

Neutrino Resonances

The transition between possible neutrino states occur at some preferred regions, called resonance regions, which are characterized by the equality between two Hamiltonian's diagonal elements. Thus the possible transitions are of two kinds: the MSW kind occurring due to changing electronic density when both diagonal elements corresponds to two neutrino states or two anti-neutrino ones, and the RSFP kind corresponding to resonant spin flavor in presence of a magnetic field [7] and involving a neutrino and a anti-neutrino state of different flavors. In general we expect 4 significant resonances, two of each kind namely: the known two MSW ones which are called L and H transitions, and the corresponding RSFP ones which we call \bar{L} and \bar{H} transitions; in addition to a fifth one of RSFP kind, which we call A, but which doesn't affect the neutrino dynamics. Let us see how we can deduce these four resonances from general considerations on the full matrix. Starting from the 6×6 matrix with its six diagonal elements to be equated two by two, we have $C_6^2 = 15$ combinations. Out of these 15 combinations, 3 can be eliminated due to the Majorana character which doesn't allow for the like-flavor spin flip, 2 can be further eliminated due to the smallness of the ν_{μ} - ν_{τ} potential difference and likewise for $\bar{\nu}_{\mu}$ - $\bar{\nu}_{\tau}$. For the remaining 10 cases, they constitute five pairs of conjugate transitions, for which there could only occur a transition from each pair at a time; since the resonance density computed by equating diagonal elements can be of both signs, while it's conjugate transition will be necessarily have the inverse sign, and since physically only the case with positive value is relevant. This leaves us with five transitions, the fifth one being as mentioned previously not significant. We will study each of the MSW and RSFP kinds separately.

MSW Resonances

In general, MSW transition between two neutrinos (or anti-neutrinos) is studied around its resonance and the general form of the 2×2 submatrix is:

$$\frac{1}{2E} \begin{pmatrix} c & b \\ b & Y_e \times z \end{pmatrix} \tag{7}$$

where $z = 2\alpha\rho E$, and the resonance corresponds to $z_{res} = \frac{c}{Y_e}$. The transition will be adiabatic, *i.e.* there is no jumping between eigenstates, for $\gamma_{res} > 1$, where γ_{res} is the adiabaticity parameter [22] at the resonance given in this case by:

$$\gamma_{res} = \left(\frac{E_{no}}{E}\right)^{\frac{2}{3}} \tag{8}$$

with

$$E_{na} = 2.74 \times 10^9 \times Y_e^{\frac{1}{2}} \times \left(\frac{|b|}{1 \,\text{eV}^2}\right)^3 \times \left(\frac{|c|}{1 \,\text{eV}^2}\right)^{-2} \,\text{MeV}$$
(9)

The parameters b and c are given by:

Mass hiera-	SNP sol-	b(L)	c(L)	b(H)	c(H)
Normal	LMA	3.29×10^{-5}	1.81×10^{-5}	8.46×10^{-5}	2.67×10^{-3}
	LOW	6.31×10^{-8}	-2.60×10^{-6}	8.53×10^{-5}	2.69×10^{-3}
Inverted	LMA	-3.29×10^{-5}	2.35×10^{-5}	-8.61×10^{-5}	-2.72×10^{-3}
	LOW	-6.13×10^{-8}	2.80×10^{-6}	8.53×10^{-5}	-2.69×10^{-3}

b and c are given in eV^2 . The sign (-) for the c value means that the conjugate transition occurs instead of the usual one, for example in the case of inverted mass hierarchy within LMA solution, $c(H)=-2.7\times 10^{-3}\,\mathrm{eV}^2$ means that $\bar{\nu}_1\longleftrightarrow\bar{\nu}_3$ occurs instead of $\nu_1\longleftrightarrow\nu_3$ ⁵.

The values of E_{na} are given in MeV at each layer within all scenarios by:

Mass hierarchy	SNP solution	L	H
Normal	LMA	2.11×10^{5}	164. 6
Worman	LOW	7.20×10^{-2}	166. 2
Inverted	LMA	$\it 1.25\times10^{5}$	167. 2
muentea	LOW	5.69×10^{-2}	166. 2

RSFP Resonances

RSFP transitions occurring between a neutrino state and an anti-neutrino one is also studied around its resonance and is of the form:

$$\frac{1}{2E} \begin{pmatrix} c & sz \\ sz & dz \end{pmatrix} \tag{10}$$

but with $s = \frac{\mu B}{\alpha \rho} \simeq 1.9 \times 10^{-9} \times (\frac{\mu B_{\perp o}}{\mu_B G})$. Likewise, we find that the adiabaticity parameter is given as in Eq. (8), but with

$$E_{na} = 1.89 \times 10^{-17} \times d^{-\frac{5}{2}} \times \left(\frac{|c|}{1 \,\text{eV}^2}\right) \times \left(\frac{\mu B_{\perp o}}{\mu_B G}\right)^3 \,\text{MeV}$$
(11)

where $d = 1-2Y_e$ for both \bar{L} and \bar{H} , $d=1-Y_e$ for A. Note that E_{na} is proportional to $(\mu B_{\perp o})^3$, which shows that the adiabaticity of the RSFP resonances depends strongly on the interaction term $\mu B_{\perp o}$. The values of c is given in eV^2 .

Mass hierarchy	SNP solution	$c~(\bar{L})$	$c~(\bar{H})$	c(A)
Normal	LMA	1.81×10^{-5}	2.67×10^{-3}	2.65×10^{-3}
	LOW	-2.60×10^{-6}	2.69×10^{-3}	2.71×10^{-3}
Inverted	LMA	2.35×10^{-5}	-2.72×10^{-3}	-2.74×10^{-3}
mverted	LOW	2.80×10^{-6}	-2.69×10^{-3}	-2.71×10^{-3}

⁵Note that the L resonance transition occurs in the antineutrino channel for the case of normal mass hierarchy within the LOW scheme (For more details see $Appendix\ A$).

Fig 2: The dependence of the flip probability on the neutrino energy.

We give in the following table, the values of E_{na} in MeV multiplied by $(\frac{\mu B_{\perp o}}{\mu_B G})^{-3}$ for \bar{L} and \bar{H} , and by $(\frac{\mu_{\mu\tau}B_{\perp o}}{\mu_B G})^{-3}$ for A, at each layer within all scenarios:

Mass hierarchy	SNP solution	$ar{L}$	$ar{H}$	A
Normal	LMA	3.38×10^{-11}	4.99×10^{-9}	2.83×10^{-19}
	LOW	4.86×10^{-12}	5.02×10^{-9}	2.90×10^{-19}
Inverted	LMA	4.39×10^{-11}	5.08×10^{-9}	2.93×10^{-19}
mvertea	LOW	5.23×10^{-12}	5.02×10^{-9}	2.90×10^{-19}

Note that stating that the resonance corresponds to the equality of diagonal elements of Eq. (4) is not correct strictly speaking. The resonances, which corresponds to the minima of the difference between the Hamiltonian eigenvalues, match up exactly the diagonal elements when the off-diagonal elements are r-independent, which is the case for the MSW effect. On the other hand, the resonances will be shifted when the off-diagonal elements are r-dependent as in the case of the RSFP effect. In our case however where the r-dependency is of the form $\rho \propto B \sim r^{-3}$, this shift is negligeable as we show in $Appendix\ B$.

The Adiabaticity at Neutrino Resonances

At the resonance, jumping probability is given by [23]

$$P_f = exp\left\{-\frac{\pi}{2} \left[\frac{E_{na}}{E}\right]^{\frac{2}{3}}\right\} \tag{12}$$

which depends on the energy E as we see from Fig. 2.

Now the observable part of the supernova neutrino spectrum lies mainly between the energies 5 and 50 MeV and we will consider only energies in this range in our work. One can then divide the whole range of energy in three parts:

• Part I: $P_f \leq 0.1 \sim 0$, corresponding to $E_{na} \gtrsim 70 \,\mathrm{MeV}$, and where pure adiabatic conversions occurs.

- Part II: $70\,\mathrm{MeV} \gtrsim E_{na} \gtrsim 0.2\,\mathrm{MeV}$, for which $0.1 \leq P_f \leq 0.9$. In this range, P_f increases strongly with the neutrino energy. The adiabaticity is partially broken.
- Part III: $P_f \ge 0.9 \sim 1$, corresponding to $E_{na} \lesssim 0.2 \,\text{MeV}$, where the flip probability is close to 1, and which leads to a strong violation of adiabaticity.

Then one can find easily that the transition at the H resonance is completely adiabatic for all possible scenarios, as mentioned above. While, at the L resonance, the transition is: completely adiabatic within LMA scenario, and therefore $P_L \simeq 0$; and completely non-adiabatic within LOW one and therefore $P_L \simeq 1$, for both normal and inverted hierarchies.

For RSFP transitions, the adiabaticity depends on the value of $\mu B_{\perp o}$, and therefore we will divide the whole range of $\mu B_{\perp o}$ according to the adiabaticity at the \bar{H} resonance, then the $\mu B_{\perp o}$ regions are:

I – Completely non-adiabatic if: $\mu B_{\perp o} < 340 \mu_B G$.

II – Partially broken if: $340\mu_B G < \mu B_{\perp o} < 2400\mu_B G$.

III – Purely adiabatic if: $\mu B_{\perp o} > 2400 \mu_B G$.

We have plotted in Fig. 3 the flip probability at the \bar{H} layer as a function of the energy for different values of $\mu B_{\perp o}$. The curves from (1) to (6) correspond to $\frac{\mu B_{\perp o}}{\mu_B G}$ =300, 500, 1000, 1500, 2000, 2500 respectively.

The dependance of the flip probability at the layer \overline{H} , on the neutrino energy for different values of $\mu B_{\perp o}$.

At the A resonance layer, the E_{na} values are very small within the $\mu B_{\perp o}$ considered range, which corresponds to a complete non-adiabatic conversion, from which we deduce that the transition at the layer A doesn't affect the neutrino flavor dynamics. For the \bar{L} layer, the adiabaticity depends on the SNP solution and the specific mass hierarchy. Thus, if $\mu B_{\perp o}$ is larger than a given value $(\mu B_{\perp o})_2$, the transition will be purely adiabatic; if it is less than the other limiting value $(\mu B_{\perp o})_1$, the transition will be completely non-adiabatic; and finally when $\mu B_{\perp o}$ lies between these two values, the adiabaticity

will be partially broken. We give in units of $\mu_B G$, these two limiting values for the various scenarios:

Mass Hierarchy	SNP solution	$(\mu B_{\perp o})_1$	$(\mu B_{\perp o})_2$
Normal	LMA	1800	12700
NOTTHAL	LOW	3500	24300
Inquented	LMA	1700	11600
Inverted	LOW	3400	23700

Note that the $\mu B_{\perp o}$ interval where the \bar{L} (\bar{H}) adiabaticity is partially broken intersects with the similar one for the \bar{H} (\bar{L}) resonance within the LMA solution, but it doesn't within the LOW scheme. Then the region II can be divided in two parts⁶: the first one corresponds to the completely non-adiabatic resonance at the \bar{L} layer, i.e. $\mu B_{\perp o}$ lies between $340\mu_B G$ and $1800\mu_B G$ ($1700\mu_B G$) to $2400\mu_B G$, it corresponds to the partially broken adiabaticity at the layer \bar{L} .

For this purpose, we will give the level crossing for each one of different scenario, which are given in Fig's 4, 5, 6 and 7, We will check later where the transition occur, namely whether is it in the neutrino or anti-neutrino channel (for MSW), and which one of the two RSFP conjugated transitions is involved.

The hierarchy of the densities of the resonance layers (L with H, and therefore \bar{L} with \bar{H} too), leads to the factorization of the neutrino flavor dynamics, the transitions between two of resonance layers can be considered independently, and therefore each transition is reduced to a two neutrino problem [11]. Furthermore, the MSW-RSFP resonances regions non-overlapping condition, for $L-\bar{L}$ or $H-\bar{H}$ transitions, is given by [24]

$$L_{\rho} \left| \tan 2\theta_{\alpha\beta} \right| + \left| \frac{2\mu_{\alpha\beta}B_{\perp} (r_1)}{\left(\frac{\Delta m^2}{2E}\right)} \right| L_{\rho} \lesssim |r_2 - r_1| \tag{13}$$

where r_1 is the radial position of the $\bar{L}(\bar{H})$ resonance; and r_2 is that the L(H) one, and $L_{\rho} \equiv \left| \frac{d(\ln \rho)}{dr} \right|^{-1}$, $\theta_{\alpha\beta}$ is the mixing angle between the two flavors α and β ($\alpha, \beta = e, \mu, \tau$). This condition is satisfied for both L- \bar{L} and H- \bar{H} .

Neutrino Fluxes from Supernovae

Having constructed the level crossing for the various scenarios, we can now extract the final ν -flux in terms of F_i (or $F_{\overline{i}}$) in function of the original flux. We can then rewrite it in terms of the flavored ν -flux using the identity:

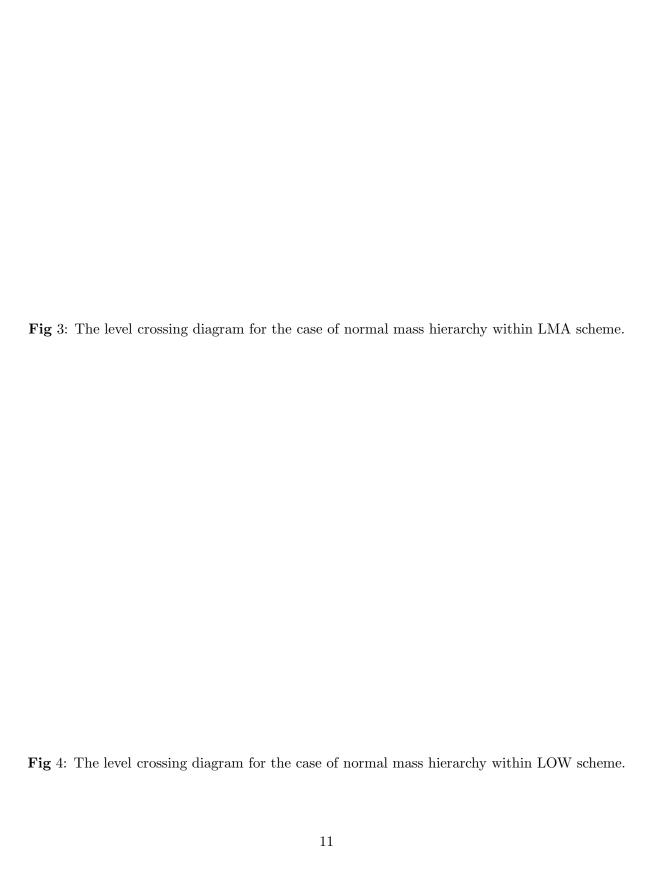
$$F_l = \sum_i |U_{li}|^2 F_i \text{ and } F_{\bar{l}} = \sum_i |U_{li}|^2 F_{\bar{i}}$$
 (14)

where $l=e,\mu,\tau$; i=1,2,3; and U_{li} are the mixing matrix elements. The final flux is thus given by the following general relation:

$$F_{i} = \sum_{l} a_{il} F_{l}^{o} + a_{i\bar{l}} F_{\bar{l}}^{o}$$

$$F_{\bar{i}} = \sum_{l} a_{\bar{i}l} F_{l}^{o} + a_{\bar{i}\bar{l}} F_{\bar{l}}^{o}$$
(15)

 $^{^6}$ We will denote them as II-a and II-b.





where a_{il} is the probability that a ν_l , which is produced inside SN core, leaves the supernova as a vacuum eigenstate ν_i . Inserting Eq. (15) in Eq. (14), we find for the flavored neutrino flux:

$$\begin{pmatrix} F_{e} \\ F_{\bar{e}}^{o} \\ 4F_{x} \end{pmatrix} = \begin{pmatrix} p_{ee} & p_{e\bar{e}} & 1 - p_{ee} - p_{e\bar{e}} \\ p_{\bar{e}e} & p_{\bar{e}\bar{e}} & 1 - p_{\bar{e}e} - p_{\bar{e}\bar{e}} \\ 1 - p_{ee} - p_{\bar{e}e} & 1 - p_{e\bar{e}} - p_{\bar{e}\bar{e}} & 2 + p_{ee} + p_{e\bar{e}} + p_{\bar{e}e} + p_{\bar{e}\bar{e}} \end{pmatrix} \begin{pmatrix} F_{e}^{o} \\ F_{\bar{e}}^{o} \\ F_{x}^{o} \end{pmatrix}$$
(16)

where p_{ee} is the survival probability of ν_e , *i.e*, the probability that a ν_e doesn't change during the core collapse; $p_{\bar{e}e}$ the probability that a ν_e leaves SN as a $\bar{\nu}_e$; the index (°) refers to the original fluxes. It is those various matrix elements which characterize the probability of SN neutrino conversion. Those probabilities satisfy the condition:

$$\sum_{\alpha} p_{\alpha\beta} = \sum_{\beta} p_{\alpha\beta} = 1 \tag{17}$$

which are functions of the probabilities a_{il} s and U_{ei} s, and $\alpha,\beta=e,\overline{e},x$.

Case of Normal Mass Hierarchy

For the LMA scheme: We find from the level crossing for the case of the normal mass hierarchy (Fig. 4), that the final flux is given by

$$F_{1} = (1 - p_{\bar{L}})p_{\bar{H}}F_{\bar{e}}^{o} + (1 - (1 - p_{\bar{L}})p_{\bar{H}})F_{x}^{o}, F_{2} = (1 - p_{\bar{H}})F_{\bar{e}}^{o} + p_{\bar{H}}F_{x}^{o}$$

$$F_{3} = F_{e}^{o}, F_{\bar{1}} = p_{\bar{H}}p_{\bar{L}}F_{\bar{e}}^{o} + (1 - p_{\bar{H}}p_{\bar{L}})F_{x}^{o}, F_{\bar{2}} = F_{x}^{o}, F_{\bar{3}} = F_{x}^{o}$$

$$(18)$$

then the SN ν -conversion probabilities are given by

$$p_{ee} \simeq 10^{-3}, \ p_{e\bar{e}} \simeq 0.65 \times (1 - p_{\bar{L}}) \, p_{\bar{H}} + 0.35 \, (1 - p_{\bar{H}})$$

$$p_{\bar{e}e} \simeq 0, \ p_{\bar{e}\bar{e}} \simeq 0.65 \times p_{\bar{L}} p_{\bar{H}}$$
(19)

For the LOW scheme: According to Fig. 5, the final flux with the LOW scheme is given by

$$F_{1} = p_{\bar{H}}F_{x}^{o} + (1 - p_{\bar{H}})F_{\bar{e}}^{o}, \quad F_{2} = F_{x}^{o}, \quad F_{3} = p_{\bar{L}}F_{e}^{o} + (1 - p_{\bar{L}})F_{x}^{o}$$

$$F_{\bar{1}} = p_{\bar{H}}F_{\bar{e}}^{o} + (1 - p_{\bar{H}})F_{x}^{o}, \quad F_{\bar{2}} = (1 - p_{\bar{L}})F_{e}^{o} + p_{\bar{L}}F_{x}^{o}, \quad F_{\bar{3}} = F_{x}^{o}$$

$$(20)$$

and therefore the SN ν -conversion probabilities are

$$p_{ee} \simeq 10^{-3} \times p_{\bar{L}}, \ p_{e\bar{e}} \simeq 0.64 \times (1 - p_{\bar{H}})$$

 $p_{\bar{e}e} \simeq 0.36 \times (1 - p_{\bar{L}}), \ p_{\bar{e}\bar{e}} \simeq 0.64 \times p_{\bar{H}}$ (21)

Case of Inverted Mass Hierarchy

For the LMA scheme: The final flux is given in this case (See Fig. 6) by:

$$F_{1} = p_{\bar{H}}F_{x}^{o} + (1 - p_{\bar{H}})F_{\bar{e}}^{o}, \quad F_{2} = F_{x}^{o}, \quad F_{3} = p_{\bar{L}}F_{e}^{o} + (1 - p_{\bar{L}})F_{x}^{o}$$

$$F_{\bar{1}} = p_{\bar{L}}F_{x}^{o} + (1 - p_{\bar{L}})F_{e}^{o}, \quad F_{\bar{2}} = (1 - p_{\bar{H}})F_{x}^{o} + p_{\bar{H}}F_{\bar{e}}^{o}, \quad F_{\bar{3}} = F_{x}^{o}$$

$$(22)$$

the SN ν -conversion probabilities are given by

$$p_{ee} \simeq 10^{-3} \times p_{\bar{L}}, \ p_{e\bar{e}} \simeq 0.65 \times (1 - p_{\bar{H}})$$

 $p_{\bar{e}e} \simeq 0.65 \times (1 - p_{\bar{L}}), \ p_{\bar{e}\bar{e}} \simeq 0.35 \times p_{\bar{H}}$ (23)

For the LOW scheme: We find for the final flux from Fig. 7:

$$F_{1} = p_{\bar{L}} F_{e}^{o} + (1 - p_{\bar{L}}) F_{x}^{o}, \quad F_{2} = F_{x}^{o}, \quad F_{3} = (1 - p_{\bar{H}}) F_{\bar{e}}^{o} + p_{\bar{H}} F_{x}^{o}$$

$$F_{\bar{1}} = p_{\bar{L}} F_{x}^{o} + (1 - p_{\bar{L}}) F_{e}^{o}, \quad F_{\bar{2}} = (1 - p_{\bar{H}}) F_{x}^{o} + p_{\bar{H}} F_{\bar{e}}^{o}, \quad F_{\bar{3}} = F_{x}^{o}$$

$$(24)$$

and the SN ν -conversion probabilities are given by:

$$p_{ee} \simeq 0.64 \times p_{\bar{L}}, \ p_{e\bar{e}} \simeq 10^{-3} \times (1 - p_{\bar{H}})$$

 $p_{\bar{e}e} \simeq 0.64 \times (1 - p_{\bar{L}}), \ p_{\bar{e}\bar{e}} \simeq 0.36 \times p_{\bar{H}}$ (25)

Note that any significant value for $p_{e\bar{e}}$ or $p_{\bar{e}e}$, is a strong signature of the spin flavor precession effect on the SN neutrino dynamics.

4 Neutrino Conversion Effects on the Mass Spectrum

Let us discuss the signatures of the various scenarios as far as the emerging neutrino signal, as well as their discriminative power at the future neutrino detectors.

For future supernova neutrino burst, the present detectors can gives, for a typical supernova, at Super-Kamiokande [2] about 5000 ν_e events, and a few hundred events can be detected in both SNO [3], LVD [25] and MACRO [4]. In this paper, we are interested on the features of the final neutrino spectra that are required for the identification of the neutrino mass spectra. The effects of neutrino mixing and magnetic moment on the final neutrino spectra can be observed through: a) the partial or complete disappearance/appearance of the ν_e neutronization peak, b) the appearance of soft, hard or composite spectra of ν_e and $\bar{\nu}_e$; and c) the Earth matter effects on both ν_e and $\bar{\nu}_e$ spectra. Let us estimate these effects on the observed spectra at the Earth detectors.

- a) Neutronization Peak: It comes at the first stage of core collapse and corresponds to a and the observed signal during the of the neutrino burst first few milliseconds duration. In the absence of neutrino conversion, the dominant signal are ν_e s, are produced by the electron capture on protons and nuclei while the shock wave passes through the neutrinosphere [14]. Since the original flux is made of ν_e , the final observed fluxes give a direct measurement of the extent of conversion of ν_e into the other neutrino species. It is thus clear that the neutronization peak is proportional to the ν_e s survival probability.
- b) The Nature of the Final Spectra: due to the difference between the interactions strengths of the various neutrino species with matter, their average energies differ and are given by [26]:

$$\langle E_{\nu_e}^o \rangle = 10 \sim 12 \,\text{MeV}, \ \langle E_{\bar{\nu}_e}^o \rangle = 14 \sim 17 \,\text{MeV}, \ \langle E_{\nu_x}^o \rangle = 24 \sim 27 \,\text{MeV}$$
 (26)

E means the original average energy (i.e. in the absence ν -conversion). Thus finding for example $\langle E_{\nu_e} \rangle > \langle E_{\bar{\nu}_e} \rangle$, would be is a signature of neutrino conversion, since it implies that the contribution of the converted original hard ν_x spectrum to the final ν_e flux is significantly larger than its contribution to the final $\bar{\nu}_e$ flux. On the other hand there is another effect which has to be accounted for: the fact that the neutrino interaction cross section increases with energy, the neutrino spectra from the

cooling stage won't be exactly thermal, but will get pinched. We can account easily for this pinching effect by parametrizing the original spectra as [26, 27]:

$$F_i^o(E) \propto \frac{E^2}{1 + \exp(E/T_i - \eta_i)} \tag{27}$$

where T_i and η_i are given by

$$T_e \approx 3 \sim 4 \,\mathrm{MeV} \,,\, T_{\overline{e}} \approx 5 \sim 6 \,\mathrm{MeV} \,,\, T_x \approx 7 \sim 9 \,\mathrm{MeV}$$

$$\eta_e \approx 3 \sim 5,\, \eta_{\overline{e}} \approx 2 \sim 2.5,\, \eta_x \approx 0 \sim 2$$

The final ν_e ($\bar{\nu}_e$) spectrum can be qualitatively divided into three types:

- 1) The original "soft" spectrum of the ν_e ($\bar{\nu}_e$) (corresponding to the survival probability $p_{ee}=1$ ($P_{\bar{e}\bar{e}}=1$)).
- 2) The "hard" spectrum of ν_x (corresponding to the survival probability $p_{ee} = p_{e\bar{e}} = 0$ ($p_{\bar{e}\bar{e}} = p_{\bar{e}e} = 0$) which would be the case when there is a complete interchange of spectra, i.e. $\nu_e \leftrightarrow \nu_x$ ($\bar{\nu}_e \leftrightarrow \nu_x$); and not $\bar{\nu}_e \leftrightarrow \nu_e$).
- 3) The "composite" spectrum, which is a mixture of the original soft and the hard spectra is comparable in proportions. There are other cases which are difficult to distinguish like the case where the ν_e ($\bar{\nu}_e$) spectrum contains only ν_e and ν_x , $\bar{\nu}_e$ and ν_x , or all species. In order to distinguish among them, we denote the spectrum containing: ν_e and ν_x by compo-1, the one containing $\bar{\nu}_e$ and ν_x by compo-2; and the one with all the species by compo-3. In some cases, the appearance of one of these case is a strong signature of the spin flavor precession effect, namely when the ν_e -spectrum contains $\bar{\nu}_e$ and vice-versa.

c) the Earth Matter Effect:

The SN neutrinos, in order to reach the detector, have to go through various amount of the Earth material. This amount depends on the direction of the SN with respect to the Earth as well as the time of the day. This effect which could modify significantly the flavor composition of the flux may be sought by comparing the signal of a future SN from detectors at different geographical locations. Certain features of the energy spectra could also reveal this effect even from the observations at one detector.

Neutrinos are expected to be arriving at the surface of the Earth as mass eigenstates (vacuum eigenstates); where they oscillate in the Earth matter, *i.e.*, they lose their coherence. The possibility of the Earth matter effect's observation depends strongly on the differences between the a_{il} and also the differences between the P_{ie} parameters (for more details, see Appendix C).

Let us now summarize the results within all previous scenarios in the following table:

5 Conclusion

We attempted in this paper to check the sensibility of the supernovae final flux of neutrinos to both the magnetic field and matter effect assuming three active neutrinos. We have taken the value of $|U_{e3}|^2$

Region	SNP solution	Neutro-	Spectrum of		Earth effects	
of $\mu B_{\perp o}$	SINF SOLUTION	Peak	$ u_e$	$ar{ u}_e$	$ u_e \bar{ u}_e$	
I	LMA normal	ν_x	hard	compo-2	× ✓	
	inverted	ν_x	hard	compo-2	× ✓	
1	LOW normal inverted	ν_x	hard	compo-2	× ✓	
		ν_e, ν_x	compo-1	compo-2	√ ✓	
	-a LMA normal	$\bar{\nu}_e, \nu_x$	compo-2	hard	√ ✓	
II	inverted	$\bar{\nu}_e, \nu_x$	compo-2	compo-2	✓ ✓	
	$\begin{array}{cc} \text{-b LMA} & \text{normal} \\ & \text{inverted} \end{array}$	$\bar{\nu}_e, \nu_x$	compo-2	compo-2	✓ ✓	
		$\bar{\nu}_e, \nu_x$	compo-2	compo-3	✓ ✓	
	$\begin{array}{c} \text{LOW} & \text{normal} \\ & \text{inverted} \end{array}$	$\bar{\nu}_e, \nu_x$	compo-2	compo-2	✓ ✓	
		ν_e, ν_x	compo-1	compo-2	✓ ✓	
III	LMA normal inverted	$\bar{\nu}_e, \nu_x$	compo-2	hard	✓ ×	
		ν_e, ν_x	compo-2	compo-2	✓ ✓	
	$egin{array}{ll} { m LOW} & { m normal} \ & { m inverted} \end{array}$	$\bar{\nu}_e, \nu_x$	compo-2	hard	✓ ✓	
		ν_e, ν_x	compo-1	compo-1	✓ ×	

Table 1: The dependance of the final spectra on: 1) the SNP solution, 2) the mass hierarchy and 3) the range of $\mu B_{\perp o}$. "soft" in the column refers to the original ν_e ($\bar{\nu}_e$) spectrum and "hard" refers to the original ν_x spectrum. In the Earth matter effect column, \checkmark and \times indicate the possibility of significant effects.

to be just below the experimental upper bound given by CHOOZ [21], which makes the transition at the H layer completely adiabatic. We then divided the whole range of values considered for $\mu B_{\perp o}$ into three regions I, II, and III according to the adiabaticity at the \bar{H} layer. We could then make some predictions on the conversion effects for supernova neutrinos. The predictions differ for the different schemes, which opens up the possibility of discriminating between them using data from future neutrino bursts. We studied the possibility of observing the conversion effects through: (i) The partial or complete change of the flavor of the neutronization peak, (ii) The appearance of a hard or composite ν_e and/or $\bar{\nu}_e$ spectra due to the conversion effect instead of their original soft spectra. (iii) the Earth matter effect from the conversion in the Earth material. We found that indeed neutrino conversion does change significantly the spectrum shape. Let us now summarize the salient features of the final flux as it appears from the last table:

- 1. The appearance of a hard $\bar{\nu}_e$ makes the mass hierarchy to be normal.
- 2. A hard ν_e spectrum makes $\mu B_{o\perp}$ to be in the first region, while a hard $\bar{\nu}_e$ spectrum exclude the first region.
- 3. The absence of the Earth matter effect in the ν_e channel implies that $\mu B_{o\perp}$ to be in the first region; while the absence in $\bar{\nu}_e$ one implies that it must be in the third region.
- 4. If $\bar{\nu}_e$ contains all spieces (i.e. ν_e , $\bar{\nu}_e$ and ν_x), the SNP solution must be LMA, the mass hierarchy is inverted and $\mu B_{\perp o}$ lies between $1700 \mu_B G$ and $2400 \mu_B G$.
- 5. If both spectra of ν_e and $\bar{\nu}_e$ contain only ν_e and ν_x , the mass hierarchy will be inverted, the SNP

solution will be LOW, and $\mu B_{\perp o}$ will be larger than $2400 \mu_B G$.

Notice that some possible observations can rule out all of the various scenarios above, like the appearance of a soft ν_e (or $\bar{\nu}_e$) signal, which would exclude all the above scenarios, since then the value of $|U_{e3}|^2$ would be less than 10^{-3} .

The final neutrino spectra can thus help in resolving three main kinds of ambiguities that remain to be resolved with the current data: (i) the solution of the SNP, (ii) the type of mass hierarchy (sign of Δm_{32}^2), and (iii) probe the magnitude of the $\mu B_{o\perp}$ value, assuming $|U_{e3}|^2$ to be 10^{-3} . The implications of the results of this work will depend on when will the next–neutrino burst from a Galactic supernova be detected. On the other hand, there is a good chance that within the next few years the present, ongoing, or future planned experiments will allow us to identify the specific solution of the solar neutrino problem considered in this work. This will significantly diminish the number of possible schemes and will allow us to further sharpen the predictions of the effects for supernovaneutrinos.

Acknowledgement

We would like to thank Francesco Vissani for useful comments on the paper.

A In which Channel does the L Resonance Occur?

Taking the Hamiltonian in the (ν_e, ν_α) basis:

$$\frac{1}{2E} \left(\begin{array}{cc} W & K \\ K & Qz \end{array} \right) \tag{29}$$

where ν_{α} is any combination of the non-electronic neutrinos, K and W are given in function of the various Δm^2 's; and Q is a function of θ_{ij} 's and Y_e . We know that the resonance occurs at $z_{res} = \frac{W}{Q}$; if $z_{res} < 0$, then the transition occurs between $(\bar{\nu}_e, \bar{\nu}_{\alpha})$ instead of (ν_e, ν_{α}) . In general Q is always positive, thus we should check the sign of W.

W represents the eigenvalues of the Hamiltonian submatrix, which corresponds to the non-electronic states (ν_{μ},ν_{τ}) . (see. Sec II); In order to probe the sign of these two values in the general case, we take a 2 × 2 symmetric matrix, similar to the mass matrix in the subspace (ν_{μ},ν_{τ}) , as follow

$$\begin{pmatrix}
\varepsilon & \lambda \\
\lambda & \sigma
\end{pmatrix}$$
(30)

where ε , λ and σ are reels; it's eigenvalues are: $\frac{1}{2}(\varepsilon + \sigma \pm \sqrt{(\varepsilon - \sigma)^2 + 4\lambda^2})$; then one can see that the two eigenvalues have:

- the same sign if $|\varepsilon\sigma| > \lambda^2$.
- different signs if $|\varepsilon\sigma| < \lambda^2$.

The small value, in absolute value, leads the resonance at the L layer, while the largest one leads to the resonance at the H layer. Thus, we are led to look at the sign of the smallest value, replacing ε , λ and σ by their values in our case, and neglecting terms multiplied by $\frac{\Delta m_{21}^2}{\Delta m_{31}^2}$, then one can find the

condition that the resonances at both L and H layers, occurs in the same channel, it can be written as

$$\sin^2 \theta_{13} \lesssim \frac{\Delta m_{21}^2}{\Delta m_{32}^2} \cos 2\theta \tag{31}$$

this condition is satisfied in the case of inverted mass hierarchy with both LMA and LOW scenarios. But for the case of normal mass hierarchy, it is satisfied only within LMA scheme.

B The Adiabaticity of Neutrino Conversion

For neutrinos traveling through a non-constant density medium, it is proved that the adiabaticity is always satisfied except for the cases around the resonance layer, where it must be studied more thoroughly. The resonance, in general, can be characterized by the matter density value ρ , and therefore the distance r from the SN center, when the difference between the two Hamiltonian eigenvalues, $\Delta H_{eff} = \left| \frac{M_2^2}{2E} - \frac{M_1^2}{2E} \right|$, is minimal, *i.e.*

$$\frac{\partial}{\partial f} \left(\Delta H_{eff} \right|_{res} = 0 \tag{32}$$

where f is either the density ρ or the travelled distance r. Considering the 2- ν scheme (Like ν_e,ν_μ) case for the MSW effect, H can be written as:

$$H = \frac{1}{2E}U\begin{pmatrix} m_1^2 & 0\\ 0 & m_2^2 \end{pmatrix}U^{\dagger} + \frac{\alpha}{2}\rho\begin{pmatrix} 3Y_e - 1 & 0\\ 0 & Y_e - 1 \end{pmatrix}$$
(33)

and the mixing matrix U, is given by

$$U = \begin{pmatrix} \cos \theta & \sin \theta \\ -\sin \theta & \cos \theta \end{pmatrix} \tag{34}$$

Neglecting the terms proportional to the unity matrix, we find

$$H = U \begin{pmatrix} 0 & 0 \\ 0 & \Delta \end{pmatrix} U^{\dagger} + \alpha \rho \begin{pmatrix} 1 & 0 \\ 0 & 0 \end{pmatrix} = \begin{pmatrix} \alpha \rho + \Delta \sin^2 \theta & \frac{\Delta}{2} \sin 2\theta \\ \frac{\Delta}{2} \sin 2\theta & \Delta \cos^2 \theta \end{pmatrix}$$
(35)

where $\Delta = \frac{m_2^2 - m_1^2}{2E}$. Then the difference between the two eigenvalues is:

$$\sqrt{(\alpha\rho - \Delta\cos 2\theta)^2 + \Delta^2\sin^2 2\theta} \tag{36}$$

which takes its minimum at

$$\rho = \frac{\Delta}{\alpha} \cos 2\theta \tag{37}$$

This corresponds to the equality of the diagonal elements.

If we try to redo the same operation but writing this time H in the vacuum state basis (ν_1, ν_2) , we find

$$H = U^{\dagger} H U = \begin{pmatrix} 0 & 0 \\ 0 & \Delta \end{pmatrix} + \alpha \rho \begin{pmatrix} \cos^2 \theta & \frac{1}{2} \sin 2\theta \\ \frac{1}{2} \sin 2\theta & \sin^2 \theta \end{pmatrix}$$
(38)

The difference between the eigenvalues takes its minimum at the same value of ρ , given in Eq. (37), because they are different representations of the same operator H, which doesn't correspond to the diagonal elements equality

$$\rho = \frac{\Delta}{\alpha \cos 2\theta} \tag{39}$$

We will obtain the same result if we write H in any other basis, *i.e.*, the minimum of ΔH_{eff} doesn't correspond the diagonal elements equality.

One can deduce that the minimum of ΔH_{eff} corresponds to the diagonal elements equality only when the off-diagonal elements are constant, *i.e.* ρ -independent which is realized only in the flavored basis. There are some cases, like the one in the presence of magnetic moment interaction, where the flavored basis is not the best basis to deduce the resonance density directly, *i.e.* by equating the diagonal elements.

Let us consider our case, from Eq. (10), the minimum of ΔH_{eff} is given by

$$\frac{1}{2E}\sqrt{(b-cz)^2 + 4s^2z^2} \tag{40}$$

which corresponds to

$$z_{res} = \frac{bc}{c^2 + 4s^2} \tag{41}$$

but we take it $\frac{b}{c}$; since $s \ll c$, then one can write

$$z_{res} \simeq \frac{b}{c} \left(1 - 7.46 \times 10^{-14} \times \left(\frac{\mu B_{\perp o}}{\mu_B G} \right)^2 \right)$$
 (42)

thus the layer radius r_{res} is corrected by Δr_{res} , where $\frac{\Delta r_{res}}{r_{res}} = -4.21 \times 10^{-5} \times \left(\frac{\mu B_{\perp o}}{\mu_B G}\right)^{\frac{2}{3}}$, then the adiabaticity parameter will be corrected by the factor

$$\xi = 1 - 1.24 \times 10^{-13} \times \left(\frac{\mu B_{\perp o}}{\mu_B G}\right)^2 \tag{43}$$

and the jumping probability becomes

$$P_f^{\text{(corrected)}} = [P_f]^{\xi} \tag{44}$$

suppose that $P_f = 0.4$, in order to be corrected by 0.1, i.e. $P_f^{(corrected)} = 0.5$, we need that the quantity $\mu B_{\perp o}$ to be larger than $1.4 \times 10^6 \mu_B G$; which is a huge value non-available in the supernovae. We conclude that this correction doesn't affect the neutrino conversion in our work, and we have thus neglected it.

C The Earth Matter Effect⁷

If neutrinos reach the Earth detectors without interacting with matter, the signal at the detectors is given by Eq. (16). Since they reach detectors through the Earth matter, the flux given by Eq. (16) will be modified in general.

⁷We are here closely following the treatment of [11], adopting it to our case by taking into account the possibility of the $\nu - \bar{\nu}$ transition. This effect is studied with more details for difference scenarios in [28].

Let P_{ie} ($P_{\bar{i}\bar{e}}$) be the probability that a vacuum mass eigenstate ν_i ($\bar{\nu}_i$) entering the Earth reaches the detector as a ν_e ($\bar{\nu}_e$). The flux of ν_e ($\bar{\nu}_e$) at the detector is

$$F_e^D = \sum_i P_{ie} F_i, \quad F_{\bar{e}}^D = \sum_i P_{\bar{i}\bar{e}} F_{\bar{i}} \tag{45}$$

Inserting F_i , we get

$$F_e^D = F_e^o \sum_i P_{ie} a_{ie} + F_{\bar{e}}^o \sum_i P_{ie} a_{i\bar{e}} + F_x^o \sum_i P_{ie} \left(1 - a_{ie} - a_{i\bar{e}}\right)$$

$$F_{\bar{e}}^D = F_e^o \sum_i P_{\bar{i}\bar{e}} a_{\bar{i}\bar{e}} + F_{\bar{e}}^o \sum_i P_{\bar{i}\bar{e}} a_{\bar{i}\bar{e}} + F_x^o \sum_i P_{\bar{i}\bar{e}} \left(1 - a_{\bar{i}e} - a_{\bar{i}\bar{e}}\right)$$

$$(46)$$

where the a's are defined in Sec. 3. Then one can write

$$p_{ee}^D = \sum_{i} P_{ie} a_{ie}, \quad p_{e\bar{e}}^D = \sum_{i} P_{ie} a_{i\bar{e}}, \quad p_{\bar{e}e}^D = \sum_{i} P_{\bar{i}\bar{e}} a_{\bar{i}e}, \quad p_{\bar{e}\bar{e}}^D = \sum_{i} P_{\bar{i}\bar{e}} a_{\bar{i}\bar{e}}$$
(47)

Similarly we have

$$F_{e} = p_{ee}F_{e}^{o} + p_{e\bar{e}}F_{\bar{e}}^{o} + (1 - p_{ee} - p_{e\bar{e}}) F_{x}^{o}$$

$$F_{\bar{e}} = p_{\bar{e}\bar{e}}F_{\bar{e}}^{o} + p_{\bar{e}e}F_{e}^{o} + (1 - p_{\bar{e}\bar{e}} - p_{\bar{e}e}) F_{x}^{o}$$
(48)

which enables us to write:

$$F_{e}^{D} = P_{ee}^{D} F_{e}^{o} + P_{e\bar{e}}^{D} F_{\bar{e}}^{o} + \left(1 - P_{ee}^{D} - P_{e\bar{e}}^{D}\right) F_{x}^{o} F_{\bar{e}}^{D} = P_{\bar{e}\bar{e}}^{D} F_{\bar{e}}^{o} + P_{\bar{e}e}^{D} F_{e}^{o} + \left(1 - P_{\bar{e}\bar{e}}^{D} - P_{\bar{e}e}^{D}\right) F_{x}^{o}$$

$$(49)$$

From those expressions we deduce:

$$F_e^D - F_e^o = (F_e^o - F_x^o) \left(P_{ee}^D - p_{ee} \right) + (F_{\bar{e}}^o - F_x^o) \left(P_{e\bar{e}}^D - p_{e\bar{e}} \right) F_{\bar{e}}^D - F_{\bar{e}}^o = (F_{\bar{e}}^o - F_x^o) \left(P_{\bar{e}\bar{e}}^D - p_{\bar{e}\bar{e}} \right) + (F_e^o - F_x^o) \left(P_{\bar{e}e}^D - p_{\bar{e}e} \right)$$
(50)

so the Earth matter effect can be quantified by the various differences $(P_{ee}^D - p_{ee})$, $(P_{e\bar{e}}^D - p_{e\bar{e}})$, $(P_{\bar{e}\bar{e}}^D - p_{\bar{e}\bar{e}})$ and $(P_{\bar{e}e}^D - p_{\bar{e}e})$, which equal;

$$P_{ee}^{D} - p_{ee} = \sum a_{ie} (P_{ie} - |U_{ei}|^{2}), \quad P_{e\bar{e}}^{D} - p_{e\bar{e}} = \sum a_{i\bar{e}} (P_{ie} - |U_{ei}|^{2})$$

$$P_{\bar{e}\bar{e}}^{D} - p_{\bar{e}\bar{e}} = \sum a_{\bar{i}\bar{e}} (P_{\bar{i}\bar{e}} - |U_{ei}|^{2}), \quad P_{\bar{e}e}^{D} - p_{\bar{e}e} = \sum a_{\bar{i}e} (P_{\bar{i}\bar{e}} - |U_{ei}|^{2})$$
(51)

One can finally write $P_{ee}^D - p_{ee}$ as

$$P_{ee}^{D} - p_{ee} = a_{1e}(P_{1e} - |U_{e1}|^2) + a_{2e}(P_{2e} - |U_{e2}|^2) + a_{3e}(P_{3e} - |U_{e3}|^2)$$
(52)

We obtain similar expressions for the other difference terms. We notice that the last term in Eq. (52) is negligeable due to the very small depth oscillation of ν_3 inside the Earth [11]

$$P_{3e} - |U_{e3}|^2 \le 10^{-3} \tag{53}$$

Taking into account the relations $\sum |U_{ei}|^2 = 1$ and $\sum_i P_{ie} = \sum P_{i\bar{e}} = 1$, one can write

$$P_{ee}^{D} - p_{ee} = (a_{2e} - a_{1e}) (P_{2e} - |U_{e2}|^{2}), \quad P_{e\bar{e}}^{D} - p_{e\bar{e}} = (a_{2\bar{e}} - a_{1\bar{e}}) (P_{2e} - |U_{e2}|^{2})$$

$$P_{\bar{e}\bar{e}}^{D} - p_{\bar{e}\bar{e}} = (a_{\bar{2}\bar{e}} - a_{\bar{1}\bar{e}}) (P_{\bar{2}\bar{e}} - |U_{e2}|^{2}), \quad P_{\bar{e}e}^{D} - p_{\bar{e}e} = (a_{\bar{2}e} - a_{\bar{1}e}) (P_{\bar{2}\bar{e}} - |U_{e2}|^{2})$$

$$(54)$$

finally, the differences $F_e^D - F_e^o$ and $F_{\bar{e}}^D - F_{\bar{e}}^o$ can be written as

$$F_e^D - F_e^o \approx \left[(F_e^o - F_x^o) \left(a_{2e} - a_{1e} \right) + \left(F_{\bar{e}}^o - F_x^o \right) \left(a_{2\bar{e}} - a_{1\bar{e}} \right) \right] \left(P_{2e} - |U_{e2}|^2 \right) F_{\bar{e}}^D - F_{\bar{e}}^o \approx \left[(F_{\bar{e}}^o - F_x^o) \left(a_{\bar{2}\bar{e}} - a_{\bar{1}\bar{e}} \right) + \left(F_{e}^o - F_x^o \right) \left(a_{\bar{2}e} - a_{\bar{1}e} \right) \right] \left(P_{\bar{2}\bar{e}} - |U_{e2}|^2 \right)$$
(55)

In general, when the signal from two detectors D_1 and D_2 are compared, we get the following flux differences:

$$F_e^{D_1} - F_e^{D_2} \simeq \left[(F_e^o - F_x^o) \left(a_{2e} - a_{1e} \right) + \left(F_{\bar{e}}^o - F_x^o \right) \left(a_{2\bar{e}} - a_{1\bar{e}} \right) \right] \left(P_{2e}^{(1)} - P_{2e}^{(2)} \right) F_{\bar{e}}^{D_1} - F_{\bar{e}}^{D_2} \simeq \left[\left(F_{\bar{e}}^o - F_x^o \right) \left(a_{\bar{2}\bar{e}} - a_{\bar{1}\bar{e}} \right) + \left(F_e^o - F_x^o \right) \left(a_{\bar{2}e} - a_{\bar{1}e} \right) \right] \left(P_{\bar{2}\bar{e}}^{(1)} - P_{\bar{2}\bar{e}}^{(2)} \right)$$

$$(56)$$

According to this relation, the difference $F_e^{D_1} - F_e^{D_2}$ ($F_{\bar{e}}^{D_1} - F_{\bar{e}}^{D_2}$) is factorized: it is proportional to the difference of the Earth oscillation probability P_{2e} ($P_{\bar{2}\bar{e}}$) at the two detectors and a function of supernovae oscillation probabilities a's and the difference in the original fluxes of ν_e ($\bar{\nu}_e$) and ν_x . Let us consider these factors separately:

1) $P_{2e}^{(1)} - P_{2e}^{(2)}$ and $P_{\bar{2}\bar{e}}^{(1)} - P_{\bar{2}\bar{e}}^{(2)}$: if the neutrino trajectory go through only the Earth's mantle, one can use a constant density approximation, which gives [11]

$$P_{2e}^{(1)} - P_{2e}^{(2)} = \sin 2\theta_{12}^{m} \sin 2(\theta_{12}^{m} - \theta_{12}) \left[\sin^{2} \left(\frac{\pi d_{1}}{L_{m}} \right) - \sin^{2} \left(\frac{\pi d_{2}}{L_{m}} \right) \right]$$

$$P_{\bar{2}\bar{e}}^{(1)} - P_{\bar{2}\bar{e}}^{(2)} = \sin 2\theta_{\bar{e}\bar{2}}^{m} \sin 2(\theta_{\bar{e}\bar{2}}^{m} - \theta_{e2}) \left[\sin^{2} \left(\frac{\pi d_{1}}{L_{m}} \right) - \sin^{2} \left(\frac{\pi d_{2}}{L_{m}} \right) \right]$$

$$(57)$$

here θ^m and L_m are the mixing angle and the oscillation length inside the Earth respectively, and d_i is the distance travelled by neutrinos inside the Earth before reaching the detector D_i .

- 2) The second factors is a summing of two-factor terms. Let us try to see how they behave:
- * $(F_e^o F_x^o)$ and $(F_{\bar{e}}^o F_x^o)$: Since the ν_e $(\bar{\nu}_e)$ spectrum is softer than the ν_x spectrum, and the luminosities of both the spectra are similar in magnitude [29], the term $(F_e^o F_x^o)$, (and therefore $(F_{\bar{e}}^o F_x^o)$), is positive at LOW energies and becomes negative at higher energies where the ν_x flux overwhelms the ν_e $(\bar{\nu}_e)$ flux. Therefore, the Earth effect has a different sign for LOW and high energies, and there exists a critical energy E_c (\bar{E}_c) , such that $F_e^o(E_c) = F_x^o(E_c)$, $(F_{\bar{e}}^o(\bar{E}_c) = F_x^o(\bar{E}_c))$, where this change of sign takes place. Since the cross section of the neutrino interactions increases with energy, the Earth effect is expected to be more significant at higher energies (if all the other factors are only weakly sensitive to the neutrino energy).
- * $(a_{2e} a_{1e})$, $(a_{\bar{2}e} a_{\bar{1}e})$, $(a_{2\bar{e}} a_{1\bar{e}})$ or $(a_{\bar{2}\bar{e}} a_{\bar{1}\bar{e}})$: They represent the differences between the a_{il} probabilities and can be extracted from Eq. (18), Eq. (20), Eq. (22) and Eq. (24). They are seen to be dependent on the mass hierarchy as well as the specific solar neutrino solution (*LMA* or *LOW*). Non vanishing values for this difference make the observation of the Earth matter effect possible.

References

- [1] Hirata. K.S et. al., Kamiokande collaboration, Phys. Rev. Lett. 58 (1987) 1490. Bionta. R.M et. al., IMB collaboration, Phys. Rev. Lett. 58 (1987) 1494.
- [2] Fukuda. Y et al., Phys. Rev. Lett. 82 (1999) 2644, K. Scholberg (for the SuperKamiokande collaboration), hep-ex/9905016.

- [3] The SNO collaboration, Nucl. Instrum. Meth. A449 (2000) 172-207, nucl-ex/9910016.
- [4] Ambrosio. M et. al., MACRO Collaboration, Astropart. Phys. 8 (1998) 123-133.
- [5] Bahcall. J.N, Krastev. P.I and Smirnov. A.Yu, Phys. Rev D 58 (1998) 096016. Krastev. P.I, hep-ph/9905458. Gonzalez-Garcia. M.C, deHolanda. P.C, Pena-Garayand. C and Valle. J.W.F, Nucl. Phys. B573 (2000) 3-26, hep-ph/9906469.
- [6] Mikheyev. S.P and Smirnov. A.Yu, Sov. J. Nucl. Phys. 42 913-17 (1985), Nuovo Cimento 9 C 17-26 (1986), Wolfenstein. L, Phys. Rev. D 17 (1978) 2369-74.
- [7] Fujikawa. K and Shrock. R.E, Phys. Rev. Lett 45 (1980) 963; Lim. C.-S and Marciano. W.J, Phys. Rev D 37 (1988) 1368.
- [8] Particle Data Group, European Physical Journal C 15 (2001) 1, hep-ex/9907037.
- [9] Nunokawa. H, Qian. Y.-Z and Fuller. G.M, astro-ph/96100209. Akhmedov. E.Kh, Lanza. A,
 Petcov. S.T and Sciama. D.W, hep-ph/9603443. Athar. H, Peltoniemi. J.T and Smirnov. A.Yu,
 Phys. Rev. D 51(1995) 6647, hep-ph/9501283. Athar. H, hep-ph/9902222.
- [10] McLaughlin. G.C, Fetter. J.M, Balantekin. A.B and Fuller. G.M, Phys. Rev. C 59 (1999) 2873-2887, astro-ph/9902106.
- [11] Dighe. A.S and Smirnov. A.Yu, Phys. Rev D 62 (2000) 033007, hep-ph/9907423.
- [12] KamLAND collaboration, Phys. Rev. Lett. 90 (2003) 021802, hep-ex/0212021.
- [13] Bethe. H.A, Rev. Mod. Phys. 62, 802 (1990).
- [14] Suzuki. H, "Supernova Neutrinos", Physics and Astrophysics of Neutrinos, eds. Fukugita. M and Suzuki. A, Springer Verlag, 1994, pp 763.
- [15] Bethe. H.A and Wilson. J.R, ApJ 295 (1985) 14.
- [16] Woosley. S.E and Weaver. T.A, Annu. Rev. Astron. Astrophys. 24, 205 (1986).
- [17] Janka. H.-T and Hillenbrandt. W, Astron. Astrophys. Suppl. 78 (1989) 375. Notzold. D, Phys. Lett. B 196 (1987) 315.
- [18] Maki. Z, Nakagawa. M and Sakata. S, Theor. Phys. 28 (1962) 870.
- [19] Botella. F.J, Lim. C.-S and Marciano. W.J, Phys. Rev. D 35 (1987) 896.
- [20] Derbin. A.I et al., JETP Lett.57, 768 (1993).
- [21] Apollonio. Met. al., Phys. Lett. B466 (1999) 415-430, the CHOOZ collaboration, hep-ex/9907037.
- [22] Mikheyev. S.P and Smirnov. A.Yu, Sov. J. Nucl. Phys. 42 (1985) 913.

- [23] Landau. L, Phys. Z. Sowjetunion 2 (1932) 46. Zener. C, Proc. R. Soc. London, Ser. A 137 (1932) 696.
- [24] Akhmedov. E.Kh, Sov. Phys. JETP 68 (1989) 690.
- [25] Aglietta. G et. al., LVD Collaboration, Nuovo Cim. 18 C (1995) 629.
- [26] Raffelt. G.G, "Stars as Laboratories for Fundamental Physics", The University of Chicago Press, 1996.
- [27] Janka. H.-T and Hillenbrandt. W, Astron. Astrophys. Suppl. 78 (1989) 375.
- [28] Lunardini. C, Smirnov. A.Yu, Nucl. Phys. B 616 (2001) 307-348, hep-ph/0106149. Phys. Rev. D 63 (2001) 073009, hep-ph/0009356.
- [29] Janka. H.-T, Astropart. Phys. 3 (1995) 377-384, astro-ph/9503068.

This figure "Fig1ab.jpg" is available in "jpg" format from:

This figure "Fig2.jpg" is available in "jpg" format from:

This figure "Fig3.jpg" is available in "jpg" format from:

This figure "Fig4a.jpg" is available in "jpg" format from:

This figure "Fig4b.jpg" is available in "jpg" format from:

This figure "Fig5a.jpg" is available in "jpg" format from:

This figure "Fig5b.jpg" is available in "jpg" format from: